



## Study of the Effect of Adding Nano Carbon on the Structural Properties of Aluminum Pistons Manufactured Using Powder Technology

Shahad Mozar Sameen<sup>1</sup>  , Ibrahim Khalaf Salman<sup>2</sup>  

<sup>1,2</sup>Department of Physics, College of Education for Pure Science, University of Tikrit, Tikrit, Iraq

Received: 18 Feb. 2025 Received in revised forum: 14 Mar. 2025 Accepted: 26 Mar. 2025

Final Proof Reading: 25 May. 2025 Available online: 25 Dec. 2025

### ABSTRACT

The structural properties of carbon-reinforced aluminum compounds with different weight ratios (0, 0.01, 0.02 g) of carbon in aluminum pistons prepared by powder metallurgy were studied. X-ray diffraction (XRD) results were conducted for the pistons under study. The results showed that the formed crystals were polycrystalline and had a cubic structure with a preferential orientation along the (111) plane. It was found that the diffraction peaks improved, indicating greater microstructural homogeneity with increasing reinforcing ratios. The crystallite size (Cs) of the samples was also calculated and found to decrease with increasing nanocarbon support. The surfaces of the samples were also examined using scanning electron microscopy (SEM), which revealed grain growth and distribution, as well as variations in surface morphology resulting from the nanocarbon reinforcement process.

**Keywords:** Aluminum pistons, Powder technology, Reinforcement ratio, Structural Properties

Name: Shahad Mozar Sameen

E-mail: [Sm230079pep@st.tu.edu.iq](mailto:Sm230079pep@st.tu.edu.iq)



©2025 THIS IS AN OPEN ACCESS ARTICLE UNDER THE CC BY LICENSE  
<http://creativecommons.org/licenses/by/4.0/>

## دراسة تأثير إضافة الكربون النانوي على الخصائص التركيبية لمكبوسات الألمنيوم المصنعة بطريقة

### تكنولوجي المساحيق

شهد موزر سمين، ابراهيم خلف سلمان

قسم الفيزياء، كلية التربية للعلوم الصرفة، جامعة تكريت، تكريت، العراق

### الملخص

تم دراسة الخواص التركيبية لمركبات الألمنيوم المدعمة بالكربون بنسب وزنية مختلفة وهي (0, 0.01, 0.02 g) من الكربون في مكبوسة الألمنيوم المحضرة بطريقة ميتالورجيا المساحيق، وتم إجراء فحوصات حيود الأشعة السينية (XRD) لمكبوسات قيد الدراسة، وأظهرت النتائج أن البلورات المكونة كانت متعددة التبلور وذات تركيب مكعب ذو اتجاه قضيلي (111)، وتبين أن هناك تحسن في قمم الحيود وهذا يدل على تجانس البنية المجهرية بزيادة نسب التدعيم، كما تم حساب الحجم البلوري (Cs) للعينات والذي تبين أنه يقل بزيادة التدعيم بالكربون النانوي. كم تمت دراسة أسطح العينات من خلال فحص المجهر الإلكتروني الماسح (SEM) والذي بين نمو وتوزيع الحبيبات والذي أظهر تبايناً في أشكال سطوح العينات نتيجة لتأثيرها بعملية التدعيم بالكربون النانوي.

### INTRODUCTION

Composites consist of two or more phases bonded together; the first is called the matrix, which contains a material with a lower density, such as aluminum (Al). The second is reinforcement, typically in the form of particles, filaments, or fibers. Various micro- and nanoreinforcements are employed, each with distinct effects on the properties of certain Al-based composites. Common micro-reinforcements include Al<sub>2</sub>O<sub>3</sub> and others; nano-sized reinforcements include carbon nanotubes, SiC nanoparticles, and ZrO<sub>2</sub> nanoparticles<sup>(1)</sup>. Each micro-reinforcement in the Al-based composite enhances specific properties, as the reduced size of the nano-reinforcement facilitates better interfacial interaction with the matrix and can improve the resulting composite's mechanical properties<sup>(2)</sup>. The demand for lightweight, high-strength materials has increased over the past two decades across various engineering sectors<sup>(3)</sup>. To meet this demand, it is necessary to modify the material's physical properties and implement advanced thermo-

mechanical treatments. While conventional metals and alloys show a compromise between strength, weight and ductility, metal-based composites offer excellent mechanical properties along with reduced weights, which is why they are used in a wide range of engineering applications such as automobiles, ships, etc.<sup>(4)</sup>. Metal-based composites have some excellent properties such as temperature stability, thermal conductivity, higher strength and stiffness, and lower coefficient of thermal expansion, which are otherwise difficult to obtain from a single metal or homogeneous alloys<sup>(5)</sup>. Aluminum composites exhibit distinctive properties, including high stiffness, good damping, excellent thermal and thermal management properties, low density due to their light weight, and good corrosion resistance<sup>(6)</sup>. The use of pure aluminum remains very limited in engineering applications because it is soft, weak, and exhibits poor mechanical properties. Therefore, research has long focused on improving the mechanical properties of aluminum through alloying<sup>(7)</sup>. Powder technology is a simple, low-cost

method that has demonstrated effectiveness in dispersing reinforcements homogeneously within the aluminum matrix, thereby improving mechanical properties <sup>(8)</sup>. The research aims to examine the effect of nanocarbon support on the structural properties of aluminum and to assess improvements in this material's hardness, light weight, and porosity for future applications.

## MATERIALS AND METHODS

In this research, Al and carbon nanoparticle powders with sizes ranging from 10 to 20 nm (**Figure 1**) were used at different weight ratios, as shown in **Table 1**. The structural tests included XRD and SEM.

**Table 1: Weight ratios of the powders under study.**

| Samples | S1  | S2   | S3   |
|---------|-----|------|------|
| Al      | 100 | 0.99 | 0.98 |
| C       | 0.0 | 0.01 | 0.02 |

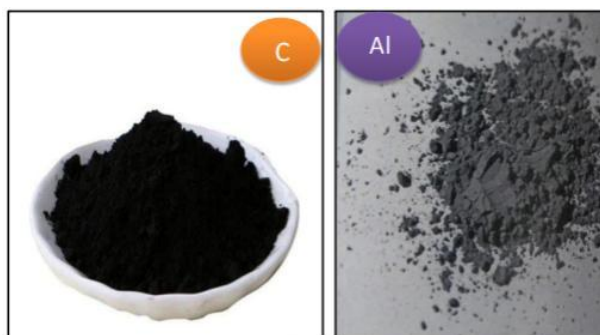


**Fig. 1: Aluminum and carbon powders.**

## EXPERIMENTAL PART

The required powder ratios were weighed out to 2 g in an agate mortar, and the ingredients were manually mixed for 30 min to achieve a homogeneous mixture. During mixing, ethyl alcohol ( $\text{CH}_3\text{OH}$ ) was added to prevent powder particles from flying and to ensure homogeneity of the mixture. The mixture was then placed in an oven at 100 °C for 10 minutes to remove the alcohol added during mixing. After mixing was complete and a homogeneous mixture was obtained, the powders were pressed using a hydraulic press. The mold was carefully placed under the press, and a pressure of 8 tons was applied for 3 minutes. After

that, the pressure was removed, and the press was lifted from the mold, which was circular in shape with a mass of (2 g), a diameter of (10 mm) and a thickness of (15 mm). After model pressing, the alloys are not ready for testing due to their low strength; therefore, they must be handled with caution during transfer to the oven. The sintering process is carried out in an oven that reaches the highest temperature (1200 °C). The alloys were placed in a clay container, and one cm-thick layer of iron filings was placed at the bottom. The alloys were placed and covered with a 1.5 cm layer of silica (red sand) and a layer of iron filings to prevent oxidation during sintering. The container was closed with a layer of refractory clay. The container was placed in the oven, and the temperature was raised to the annealing temperature of 520 °C for one hour. The samples were left in the oven overnight to cool to room temperature, after which they were removed from the crucible.

## RESULTS AND DISCUSSION

### a. X-ray diffraction (XRD):

The results of XRD showed that the pure aluminum pistons reinforced with nanocarbon are polycrystalline nature and have a cubic structure, i.e. the crystal lattice constants are ( $a = b = c$ ), and the presence of diffraction peaks corresponding to the levels (311), (220), (200), and (111) is observed at angles ( $2\theta = 38.64, 44.70, 65.07$ , and  $78.19$ ) respectively, and in the preferential direction (111). When comparing these results with the International Card (ICDD) number (04-0787), it was found that the results are largely consistent. As shown in **Figure 2**, XRD results indicate improved diffraction peaks, indicating a more homogeneous microstructure with increasing reinforcement ratios <sup>(9)</sup>. We notice a very small shift in some peak locations towards short wavelengths, because impurities play a major role within the crystal structure as they work to change most of the physical properties so that they can affect the distance between the crystal planes and size, which causes the peak locations to shift to

larger or smaller values. The shifts in peak locations to decimal places after the decimal point indicate stress resulting from the entry of impurity atoms, their diffusion in a similar material, and their occupation of lattice sites<sup>(10)</sup>. The average crystallite size was calculated using the Depay Shearer relation

and was found to decrease with increasing nanocarbon reinforcement. <sup>(11)</sup> As shown in Table 2, the peak width is approximately midway along the curve. Full width at half maximum (FWHM) increases as the crystal size is inversely proportional to the FWHM. <sup>(12)</sup>.

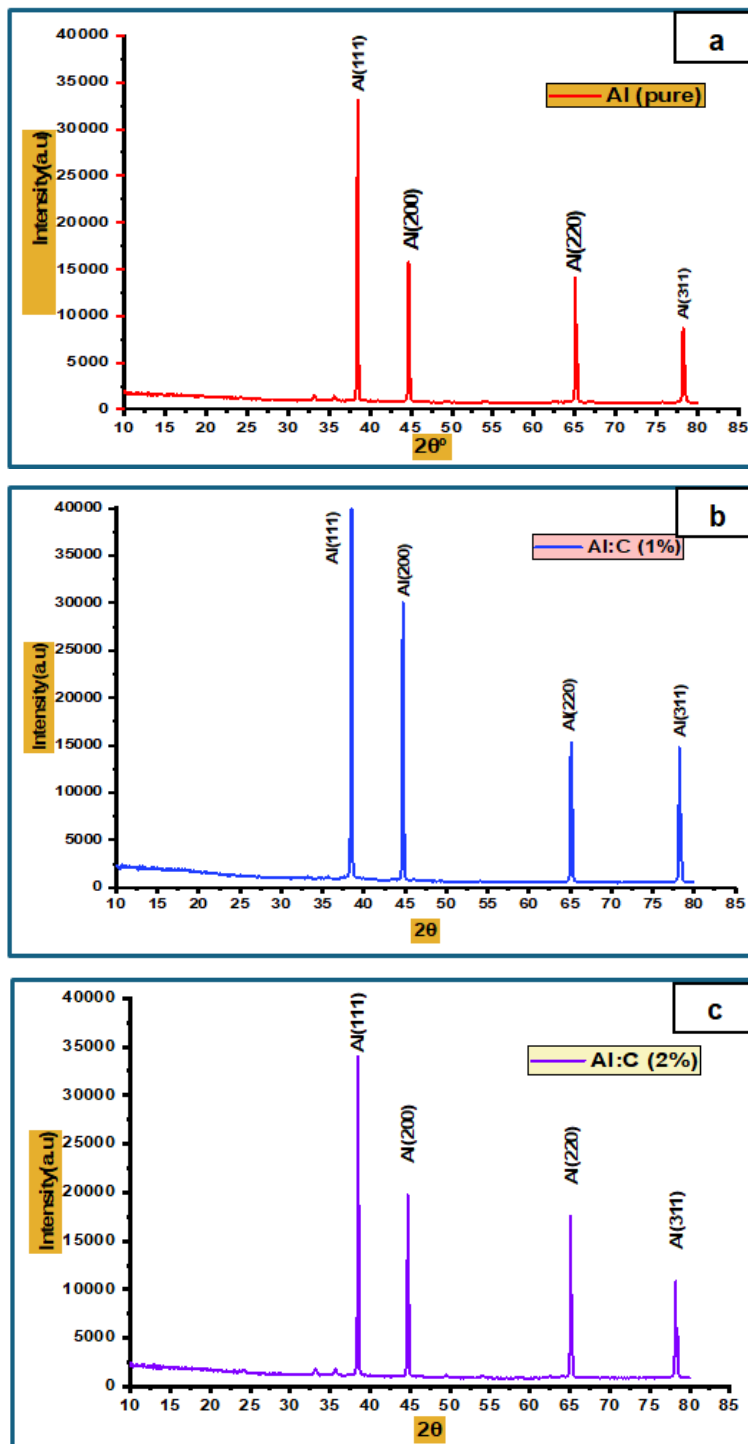


Fig. 2: XRD of the prepared aluminum pistons: a) pure, b) reinforced with 1 % of nanocarbon, c) reinforced with 2 % of nanocarbon.

Table 2: Results of XRD analysis.

| Sample           | 2θ (deg) | d (Å) | hkl | FWHM (rad) | Crystal size (nm) | Average of Crystal size (nm) | Peak |
|------------------|----------|-------|-----|------------|-------------------|------------------------------|------|
| Al: Pure         | 38.64    | 2.33  | 111 | 0.093      | 15.8              | 14.7                         | Al   |
|                  | 44.70    | 2.02  | 200 | 0.123      | 12.2              |                              | Al   |
|                  | 65.07    | 1.43  | 220 | 0.101      | 16.2              |                              | Al   |
|                  | 78.19    | 1.22  | 311 | 0.123      | 14.5              |                              | Al   |
| Al : C<br>1 % Wt | 38.45    | 2.33  | 111 | 0.175      | 8.4               | 13.8                         | Al   |
|                  | 44.70    | 2.02  | 200 | 0.096      | 15.6              |                              | Al   |
|                  | 65.07    | 1.43  | 220 | 0.098      | 16.8              |                              | Al   |
|                  | 78.20    | 1.22  | 311 | 0.126      | 14.1              |                              | Al   |
| Al : C<br>2 % Wt | 38.43    | 2.33  | 111 | 0.137      | 10.7              | 12.2                         | Al   |
|                  | 44.69    | 2.02  | 200 | 0.126      | 11.9              |                              | Al   |
|                  | 65.07    | 1.43  | 220 | 0.127      | 12.9              |                              | Al   |
|                  | 78.20    | 1.22  | 311 | 0.132      | 13.5              |                              | Al   |

#### b. Scanning Electron Microscope (SEM):

SEM was used to examine the surface morphology of pure and carbon-reinforced Al pistons (reinforcement ratio = 1.2 wt% %), to identify the nature of the surface, and to observe changes in crystal size with varying reinforcement ratios. SEM results showed changes in shape and surface structure attributable to nanocarbon reinforcement (13). In pure aluminum pistons, we observe the formation of flat, interlocking crystals with curved faces that form cavities or small networks, attributable to the nature of the interaction between nanocarbon and aluminum and to the preparation conditions. The bonding is homogeneous and random, with some surface defects and pores in the microstructure (14). When reinforced with (1.2 wt%), carbon nanoparticles begin to appear clearly and

show a homogeneous distribution with increasing reinforced ratios, as shown in Figure 3. The white color in the figures indicates a high powder density, as carbon forms shiny, flat-faced crystals. In contrast, the black appearance of the ground indicates low-density areas (15). The average particle size ranges between (20-90 nm), which is consistent with the results of researchers (16). We observed that the addition of carbon nanoparticles affected reflection and refraction, thereby improving image quality and visual details of the crystal structure under the scanning electron microscope. In addition, mixing carbon with aluminum improves scanning electron microscopy's ability to monitor crystal structure with higher accuracy, as it facilitates imaging and enables clearer identification of crystal shapes (17).

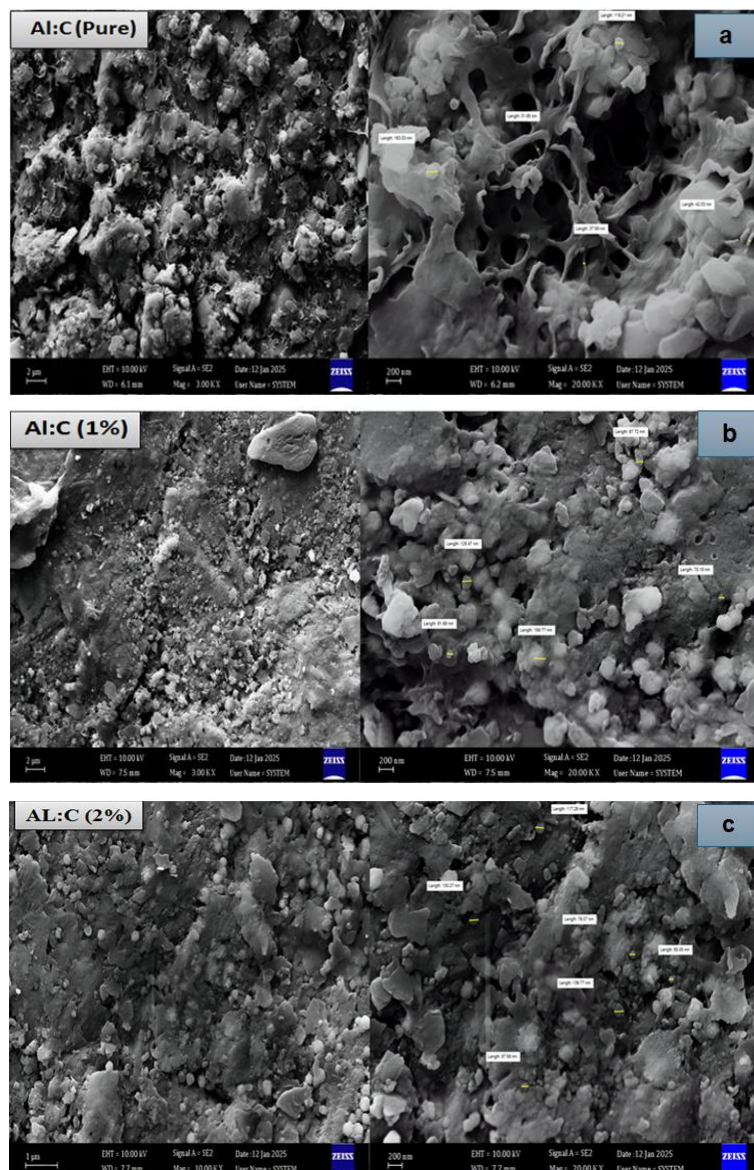


**Fig. 3: SEM images of the prepared aluminum pistons: a) pure, b) reinforced with 1 % of nanocarbon, c) reinforced with 2 % of nanocarbon.**

## CONCLUSIONS

In this study, the results of XRD showed that the pure aluminum pistons reinforced with nanocarbon are of a polycrystalline nature with a cubic structure, and with a preferential direction (111), and that the average crystal size (Cs) decreases with increasing reinforcement with nanocarbon and its value ranges between (12-15 nm). Additionally, scanning electron microscopy (SEM) revealed changes in shape and surface structure resulting from reinforcement, as well as the formation of clear spherical crystals of varying sizes and a regular

distribution of complex elements at high reinforcement ratios.

**Conflict of interest:** The authors declared no conflicts of interest.

**Sources of funding:** This research did not receive any specific grant from funding agencies in the public, commercial, or not-for-profit sectors.

**Author contribution:** Authors contributed equally to the study.

## References

1. Rajak DK, Pagar DD, Kumar R, Pruncu CI. Recent progress of reinforcement materials: a

comprehensive overview of composite materials. Journal of Materials Research and Technology. 2019;8(6):6354-74.

<https://doi.org/10.1016/j.jmrt.2019.09.068>

2. Hossain S, Rahman MM, Chawla D, Kumar A, Seth PP, Gupta P, et al. Fabrication, microstructural and mechanical behavior of Al-Al<sub>2</sub>O<sub>3</sub>-SiC hybrid metal matrix composites. Materials Today: Proceedings. 2020;21:1458-61.

<https://doi.org/10.1016/j.matpr.2019.10.089>

3. Mahmood NJ. The effect of adding different percentages of Copper on the corrosion of pure Aluminum. Tikrit J Pure Sci. 2018;2:123-8.

<http://dx.doi.org/10.25130/tjps.23.2018.037>

4. Jamwal A, Prakash P, Kumar D, Singh N, Sadasivuni KK, Harshit K, et al. Microstructure, wear and corrosion characteristics of Cu matrix reinforced SiC-graphite hybrid composites. Journal of Composite Materials. 2019;53(18):2545-53.

<https://doi.org/10.1177/0021998319832961>

5. Shaheen MA, Presswood R, Afshan S, editors. Application of Machine Learning to predict the mechanical properties of high-strength steel at elevated temperatures based on the chemical composition. Structures; 2023: Elsevier.

<https://doi.org/10.1016/j.istruc.2023.03.085>

6. Zhou M, Ren L, Fan L, Zhang Y, Lu T, Quan G, et al. Progress in research on hybrid metal matrix composites. Journal of Alloys and Compounds. 2020;838:155274.

<https://doi.org/10.1016/j.jallcom.2020.155274>

7. Rana R, Purohit R. Synthesis & analysis of mechanical and tribological behaviour of silicon carbide and graphite reinforced aluminium alloy hybrid composites. Materials Today: Proceedings. 2020;26:3152-6.

<https://doi.org/10.1016/j.matpr.2020.02.650>

8. Xiong B, Liu K, Xiong W, Wu X, Sun J. Strengthening effect induced by interfacial reaction in graphene nanoplatelets reinforced aluminum matrix composites. Journal of Alloys and Compounds. 2020;845:156282.

<https://doi.org/10.1016/j.jallcom.2020.156282>

9. Adachi H, Mizowaki H, Hirata M, Okai D, Nakanishi H. Measurement of dislocation density change during tensile deformation in coarse-grained aluminum by in-situ XRD technique with tester oscillation. Materials Transactions. 2021;62(1):62-8. <https://doi.org/10.2320/matertrans.L-M2020861>

10. Adib MH, Abedinzadeh R. Study of mechanical properties and wear behavior of hybrid Al/(Al<sub>2</sub>O<sub>3</sub>+SiC) nanocomposites fabricated by powder technology. Materials Chemistry and Physics. 2023;305:127922.

<https://doi.org/10.1016/j.matchemphys.2023.127922>

11. Ali MH. Calculation of the Atomic Scattering Factor For X-rays in Copper. Tikrit Journal of Pure Science. 2017;22(8):151-4.

<http://dx.doi.org/10.25130/tjps.24.2019.076>

12. Dalbauer V, Kolozsvári S, Ramm J, Koller C, Mayrhofer P. In-situ XRD studies of arc evaporated Al-Cr-O coatings during oxidation. Surface and Coatings Technology. 2019;358:934-41.

<https://doi.org/10.1016/j.surfcoat.2018.12.012>

13. Rikhtegar F, Shabestari S, Saghafian H. The homogenizing of carbon nanotube dispersion in aluminium matrix nanocomposite using flake powder metallurgy and ball milling methods. Powder technology. 2015;280:26-34.

<https://doi.org/10.1016/j.powtec.2015.04.047>

14. Yusuf SI, Mohammad SJ, Ali MH. Study Of The Structural Properties Of Al-Zn Compounds Manufactured By Powder Technology And Copper-Reinforced. Tikrit Journal of Pure Science. 2024;29(2):45-

52. <https://doi.org/10.25130/tjps.v29i2.1493>

15. Hong H, Yang P, Gui X, Yang Y, Liu X, Ding J, et al. Enhancing the durability of Ti-Al-C coatings: The role of powder composition and processing variables. Journal of Materials Research and Technology. 2025;34:2956-63.

<https://doi.org/10.1016/j.jmrt.2024.12.226>

16. Mehrizi MZ, Beygi R, Velashjerdi M, Nematzadeh F. Mechanically activated combustion synthesis of Ti<sub>3</sub>AlC<sub>2</sub>/Al<sub>2</sub>O<sub>3</sub> nanocomposite from

TiO<sub>2</sub>/Al/C powder mixtures. Advanced Powder Technology. 2019;30(2):311-6.

<https://doi.org/10.1016/j.apt.2018.11.007>

17. Rashad M, Pan F, Tang A, Asif M. Effect of graphene nanoplatelets addition on mechanical

properties of pure aluminum using a semi-powder method. Progress in Natural Science: Materials International. 2014;24(2):101-8.

<https://doi.org/10.1016/j.pnsc.2014.03.012>